Conformation of the Lithium Ion Complex of Antamanide, a Cyclic Decapeptide and Ion Carrier, in the Crystalline State

Isabella L. Karle

Contribution from the Laboratory for the Structure of Matter, Naval Research Laboratory, Washington, D. C. 20375. *Received January 8, 1974*

Abstract: An X-ray diffraction analysis of a single crystal of the Li^+ complex of antamanide, *cyclo*(Val-Pro-Pro-Ala-Phe-Phe-Pro-Pro-Phe-Phe), crystallized from acetonitrile, shows the Li^+ to be pentacoordinate with four ligands to the oxygens of Val_1, Pro_3, Phe_6, and Pro_8 and the fifth ligand to the N atom of the CH_3CN. Two intraring hydrogen bonds of the $1 \rightarrow 4$ type, as well as the four Li–O ligands, make the 30-membered ring fairly rigid. Eight peptide groups are in the trans conformation while the Pro_2–Pro_3 and Pro_7–Pro_8 peptide linkages are cis. The polar moieties of the molecule are turned toward the interior while the exterior surface contains the hydrophobic side groups. Two additional solvent molecules cocrystallize in the channels formed by the complexes. The space group is $P2_1$ with $a = 11.912 \pm 0.004$, $b = 23.206 \pm 0.006$, $c = 13.864 \pm 0.003$ Å and $\beta = 110° 45' \pm 04'$.

Antamanide,[1] a cyclic decapeptide found in the poisonous green mushroom *Amanita phalloides* with the sequence

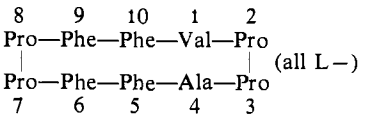

acts as an antidote to the toxin phalloidine which occurs in much larger quantities in the same mushroom. The mode of action of antamanide is not yet clearly understood but there are strong indications that the biological activity involves a membrane-tightening effect which prevents the toxin from entering the liver. Antamanide forms alkali metal complexes with a high selectivity for sodium over potassium ions[2] and the Na^+–antamanide complex is most stable in a lipophilic environment. The chief objective of the present study was to determine the conformation of an antamanide–metal ion complex. Knowledge of the conformation may aid in the understanding of the binding to the receptor sites of cell membranes and may serve as a model for ion carriers. A number of detailed spectroscopic studies have been made on the Na^+–antamanide complex in various solvents.[3–5] A preliminary account of the solid state conformation has been published.[6]

The results of the study of the molecular structure of intermediate-sized polypeptides can be useful in other areas. Since the crystals scatter X-rays very well, at least to the limit available on a four-circle diffractometer with copper radiation, the ratio of the number of measured independent reflections to the number of variables, *i.e.*, coordinates and thermal factors, is very favorable. Hence the parameters for peptide groups can be refined well and compared to those obtained for smaller peptides to determine whether any significant changes occur as the number of peptide groups increases or with folding of the backbone. These parameters may then aid in the refinement of protein molecules where the number of data is limited.

Experimental Section

Crystals of the lithium complex of antamanide were grown in acetonitrile from antamanide and LiBr. They were provided by Drs. Th. Wieland, W. Burgermeister, and H. Faulstich from the Max Planck Institut für Medizinische Forschung, Heidelberg. Since the crystals deteriorated rapidly upon drying, a crystal was sealed in a thin-walled capillary with a drop of mother liquor enclosed. Three reflections were monitored periodically during the course of the data collection and found to remain constant, thus implying that the Li^+–antamanide complex remained unaltered during the exposure to X-rays. Intensity data were collected on a four-circle automatic diffractometer with the θ–2θ scan technique using a scan of $2.0° + 2\theta(\alpha_2)° - 2\theta(\alpha_1)°$ and a scan speed of 2°/min. Lorentz and polarization corrections were made and normalized structure factors, $|E_h|$, were obtained with the aid of a K curve. The cell parameters and other pertinent data are listed in Table I.

The x and z coordinates of the Br^- ion were readily determined from a Patterson function computed with $(|E_h|^2 - 1)$ as coef-

Table I. Crystallographic Data for the Br^- Salt of the Lithium Antamanide·CH_3CN Complex Cocrystallized with Two Additional CH_3CN Molecules

Mol formula	$C_{84}H_{78}N_{10}O_{10}(LiBr)(CH_3CN)\cdot 2(CH_3CN)$
Mol wt	1357.42
Color	Colorless
Habit	Stout prism
Size, mm	$0.23 \times 0.7 \times 0.36$
Space group	$P2_1$
a, Å	11.912 ± 0.004
b, Å	23.206 ± 0.006
c, Å	13.864 ± 0.003
β, deg	$110° 45' \pm 04'$
V	3584
Z	2
Density (calcd), g/cm^3	1.258
Radiation	Cu Kα
Wave length, Å	1.54178
Linear absorption coeff, cm^{-1}	14.2
No. of independent reflections	5945

(1) See Th. Wieland in "Chemistry and Biology of Peptides," J. Meienhofer, Ed., Ann Arbor Science Publishers, Ann Arbor, Mich., 1972, pp 377–396, and references therein.

(2) Th. Wieland, H. Faulstich, W. Burgermeister, W. Otting, W. Möhle, M. M. Shemyakin, Yu. A. Ovchinnikov, V. T. Ivanov, and G. G. Malenkov, *FEBS Lett.*, **9**, 89 (1970).

(3) V. T. Ivanov, A. I. Miroshnikov, N. D. Abdullaev, L. B. Senyavina, S. F. Arkhipova, N. N. Uvarova, K. Kh. Khalilulina, V. F. Bystrov, and Yu. A. Ovchinnikov, *Biochem. Biophys. Res. Commun.*, **42**, 654 (1971); Yu. A. Ovchinnikov, V. T. Ivanov, V. F. Bystrov, and A. I. Miroshnikov, in ref 1, pp 111–116.

(4) H. Faulstich, W. Burgermeister, and Th. Wieland, *Biochem. Biophys. Res. Commun.*, **47**, 975 (1972).

(5) D. Patel, *Biochemistry*, **12**, 667 (1973). See also A. E. Tonelli, *ibid.*, **12**, 689 (1973).

(6) I. L. Karle, J. Karle, Th. Wieland, W. Burgermeister, H. Faulstich, and B. Witkop, *Proc. Nat. Acad. Sci. U. S.*, **70**, 1836 (1973).

ficients even though the Br^- ion is one of 95 atoms in the asymmetric unit and the $\Sigma Z_H^2/\Sigma Z_L^2$ ratio is only 0.31. The y coordinate for the Br^- ion was arbitrarily chosen to be $^1/_4$, a convenient value for the space group $P2_1$. For the initial E map, phases obtained from the Br^- ion alone which satisfied the criteria that $|E_h| > 1.5$ and $|F_h|_{calcd} > k|F_h|_{obsd}$, where k is the fraction of known scattering material, were used as input into the tangent formula[7,8] to compute phases for the remaining $|E_h| > 1.1$. In space group $P2_1$, phases based on one atom are necessarily real and the resulting map, characterized by a mirror plane at $y = ^1/_4$, contains atoms for both enantiomorphs. Fourteen atoms were chosen which appeared to form a reasonable fragment of one polypeptide chain and were used along with the Br^- ion to calculate an improved set of phases, obeying the criteria outlined above, for input into the tangent formula. These phases were not refined by the tangent formula but were kept constant and were used merely to extend the phase determination. Any refinement by the tangent formula under the circumstances where a relatively heavy atom is involved weights the contribution of the heavy atom in such a manner that the effect on the phases from the light atoms is lost, and the phases converge to those which would have been obtained from the heavy atom alone.[9] The second E map revealed half of the atoms of the molecule and the E map from the third cycle showed all 95 atoms in the asymmetric unit including three molecules of acetonitrile, the solvent.

The data used for the least-squares refinement were limited to the 4960 terms with $|F_o| > 5.0$. Full-matrix isotropic refinement with weighting based on counting statistics reduced the R factor to 12.1%. The program[10] and computer used allowed only 26 atoms with anisotropic thermal factors to be refined in one pass. In five passes, refining 26 atoms each time with some overlap of atoms from the previous pass, each atom was refined with anisotropic thermal factors at least once. In the interest of economy, the refinement was terminated at this point with $R = 9.0\%$. No hydrogen atoms were included in the structure factor calculations or the refinement, although a large number of hydrogen atoms were visible in difference maps.

Fractional coordinates and thermal factors for the 95 non-hydrogen atoms are listed in Table II, bond lengths and angles for the peptide chain are shown in Table III, the conformational angles[11] are listed in Table IV, while Table V contains hydrogen bond information.

Results

The Li^+–antamanide complex presents some unusual features in the conformation of the polypeptide ring and in the coordination to the metal ion. Actually, one solvent molecule becomes an integral part of the complex by making a strong ligand to the Li^+ ion. The stereodiagrams in Figure 1 show three views of the complex. Each view is at right angles to the other two views. It is immediately apparent that there is a pseudo-twofold rotation axis. An exact twofold axis is not possible since the side chains in residues 1 and 6, and 4 and 9 are different. An approximate twofold symmetry axis was indicated by spectroscopic data for the Na^+–antamanide complex in solution.[3,5]

Decapeptide Ring. The polypeptide ring, consisting of 30 atoms, is folded into a shape resembling the periphery of a saddle. Eight peptide groups are planar in the trans conformation while the Pro_2–Pro_3 and Pro_7–Pro_8 peptide linkages are in the cis conformation. Cis peptide linkages have been observed in cyclic peptides containing as many as four[12] or five[13] peptide groups; however, this structure is the first demonstration of cis peptide linkages in a cyclic polypeptide containing as many as ten peptide groups. These results for the polypeptide ring in antamanide differ from models proposed from spectroscopic data on the Na^+–antamanide complex in solution which either had all trans peptide bonds,[3] or two cis bonds between Val_1–Pro_2 and Phe_6–Pro_7.[5] Patel[5] and Tonelli[5] had considered and rejected cis bonds between Pro_2–Pro_3 and Pro_7–Pro_8 on the basis of nmr data and minimum energy calculations. In their model the conformational angles ϕ_i for residues 4, 5, 9, and 10 were nearly the same found in the crystal but the ψ_i values for these residues differed by 45–65°.

Two relatively weak intramolecular hydrogen bonds are formed between O(3)···HN(6) and O(8)···HN(1), 3.06 and 3.00 Å, which involve the following residues.

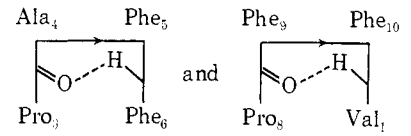

The hydrogen bonds are longer than those usually found for intermolecular O···HN bonds (2.70–2.95 Å) and not as long as the two intramolecular O···HN bonds of the type 1 → 4 found in *cyclo*(Gly-Gly-Gly-Gly-D-Ala-D-Ala) (3.04 and 3.16 Å).[14]

Conformational angles for the polypeptide ring are listed in Table IV. The largest deviation from $\omega = 0$ or 180°, a planar cis or trans peptide bond, is 8°. Figure 2 shows a plot of the ϕ, ψ angles. Residues 1, 2, 3, 6, 7, and 8 are in a low energy region as designated by Ramachandran and Sasisekharan[15] while the residues 4, 5, 9, and 10, involved in the 1 → 4 hydrogen bonding, are in a higher energy region near $\psi = 0°$. It is interesting to note that the ϕ, ψ values for the residues in the 1 → 4 hydrogen bond in *cyclo*(4Gly-2-D-Ala),[14] designated by I and IV in Figure 2, are almost the same as those found in antamanide. The ϕ, ψ values for the 1 → 4 hydrogen bond appear to be independent of the size and nature of the side groups, since in *cyclo*(4Gly-2-D-Ala), the residues involved are Gly, Gly whereas in antamanide the residues are Ala, Phe and Phe, Phe.

The folding of the chain forms a cup in which the Li^+ ion is located. Four carbonyl oxygen atoms, O(1), O(3), O(6), and O(8), form the floor of the cavity and make ligands to the Li^+. The fifth ligand involves the N atom of the solvent molecule, CH_3CN. Thus the coordination to the Li^+ is fivefold in the form of a square pyramid. The details are shown in Figure 3. The more usual coordination for Li^+ is either tetrahedral with Li···O distances near 1.96 Å or octahedral with Li···O distances near 2.16 Å. The pentacoordinate Li···O distances average 2.12 Å, an intermediate value. In the Li^+–antamanide complex all other Li···O distances are greater than 4.3 Å.

The low values for the thermal factors for the atoms in the polypeptide ring, Table II, indicate a fairly high degree of rigidity in the ring. The rigidity of the 30-

(7) J. Karle and H. Hauptman, *Acta Crystallogr.*, **9**, 635 (1956).
(8) J. Karle, *Acta Crystallogr., Sect. B*, **24**, 182 (1968).
(9) See, *e.g.*, I. L. Karle, R. D. Gilardi, A. V. Fratini, and J. Karle, *Acta Crystallogr., Sect. B*, **25**, 1469 (1969).
(10) W. R. Busing, K. O. Martin, and H. A. Levy, ORXFLS3, Oak Ridge National Laboratory, Oak Ridge, Tenn., 1971.
(11) The convention followed is that proposed by the IUPAC–IUB Commission on Biochemical Nomenclature, *Biochemistry*, **9**, 3471 (1970). In the fully extended chain $\phi_i = \psi_i = \omega_i = 180°$.
(12) J. Konnert and I. L. Karle, *J. Amer. Chem. Soc.*, **91**, 4888 (1969).
(13) H. M. Sobell, S. C. Jain, T. D. Sakore, and C. E. Nordman, *Nature (London), New Biol.*, **231**, 200 (1971).
(14) I. L. Karle, J. W. Gibson, and J. Karle, *J. Amer. Chem. Soc.*, **92**, 3755 (1970).
(15) G. N. Ramachandran and V. Sasisekharan, *Advan. Protein Chem.*, **23**, 327 (1968).

Table II. Fractional Coordinates[a] and Thermal Factors[b]

Atom	x	y	z	B_{11}	B_{22}	B_{33}	B_{12}	B_{13}	B_{23}
Br^-	0.5541	0.7500	0.4278	6.28	4.45	6.59	−1.30	2.93	−1.68
Li^+	0.5468	0.4827	0.2642	4.11	5.35	2.96	−0.08	0.15	−0.56
N(1)	0.7724	0.4764	0.5462	3.41	4.45	2.49	−0.00	0.87	0.40
C(1)	0.8510	0.5019	0.4941	4.06	4.72	3.89	−0.04	1.45	1.11
C′(1)	0.7755	0.5466	0.4192	4.32	5.42	3.19	−0.09	1.76	−0.65
O(1)	0.6708	0.5364	0.3630	3.43	4.66	3.50	−0.51	0.89	0.16
N(2)	0.8267	0.5977	0.4126	3.28	5.11	5.66	−1.14	1.22	−0.89
C(2)	0.7580	0.6400	0.3407	4.71	4.20	4.22	−0.17	0.90	0.45
C′(2)	0.7231	0.6206	0.2289	5.15	3.89	6.56	0.49	3.76	0.76
O(2)	0.8019	0.5978	0.2026	4.87	5.68	6.16	0.08	2.77	0.45
N(3)	0.6144	0.6311	0.1601	3.85	4.44	5.22	−0.36	1.68	0.54
C(3)	0.5169	0.6582	0.1858	4.09	4.68	4.89	1.11	2.32	1.44
C′(3)	0.4512	0.6127	0.2324	3.07	3.94	5.72	−0.07	0.83	0.01
O(3)	0.4381	0.5622	0.2033	4.05	3.87	5.09	−0.18	1.69	−0.82
N(4)	0.4101	0.6349	0.3022	3.75	3.68	4.39	−0.20	2.04	−0.36
C(4)	0.3567	0.5979	0.3600	4.31	3.85	3.21	−0.72	0.70	−0.32
C′(4)	0.2332	0.5711	0.2924	4.11	4.77	3.66	0.02	1.74	−0.03
O(4)	0.1983	0.5315	0.3306	5.80	7.03	4.47	−3.02	0.61	1.47
N(5)	0.1764	0.5913	0.1984	2.55	3.97	3.24	0.62	0.79	−0.52
C(5)	0.0653	0.5628	0.1322	2.26	4.94	3.17	−0.19	0.28	−0.57
C′(5)	0.0857	0.5111	0.0757	2.97	4.21	3.86	0.60	0.72	−0.41
O(5)	0.0024	0.4809	0.0243	3.24	5.15	5.29	−0.28	1.13	−1.51
N(6)	0.2033	0.4999	0.0846	3.72	3.55	3.53	0.71	1.26	−0.49
C(6)	0.2337	0.4513	0.0301	3.24	5.09	2.99	0.85	0.65	0.13
C′(6)	0.3224	0.4140	0.1079	3.72	3.69	2.75	−0.19	1.11	−0.85
O(6)	0.3977	0.4327	0.1829	3.21	4.09	3.89	0.02	0.86	−0.79
N(7)	0.3074	0.3555	0.0934	4.45	3.46	3.78	−0.31	0.92	−0.64
C(7)	0.3816	0.3169	0.1745	6.13	4.48	5.49	0.17	2.61	0.84
C′(7)	0.5156	0.3148	0.1761	8.23	4.19	3.71	2.08	2.76	0.12
O(7)	0.5329	0.3152	0.0947	7.06	6.43	4.74	1.99	2.42	0.26
N(8)	0.5996	0.3098	0.2701	5.32	6.01	3.83	2.57	3.07	0.87
C(8)	0.5856	0.3085	0.3696	6.59	3.49	4.31	1.79	2.21	0.64
C′(8)	0.5454	0.3687	0.3910	4.38	4.28	2.82	0.96	1.17	0.20
O(8)	0.5887	0.4139	0.3716	3.92	3.68	3.25	−0.09	1.49	0.45
N(9)	0.4687	0.3664	0.4433	3.42	3.43	3.54	0.48	1.39	0.08
C(9)	0.4166	0.4226	0.4598	3.50	3.88	3.33	0.18	1.78	−0.66
C′(9)	0.5073	0.4563	0.5495	6.15	4.28	3.94	−0.51	2.54	−0.50
O(9)	0.4858	0.5087	0.5552	5.72	3.92	6.60	1.15	0.05	−0.63
N(10)	0.6053	0.4301	0.6128	2.81	3.53	2.39	0.09	0.87	0.34
C(10)	0.7001	0.4611	0.6891	4.51	5.47	2.35	−0.03	0.93	−0.56
C′(10)	0.7976	0.4832	0.6456	3.72	3.91	3.53	−0.04	0.68	−0.01
O(10)	0.8877	0.5072	0.7056	5.66	6.81	4.32	−1.41	1.92	−0.87
C(11)	0.8919	0.4525	0.4342	3.65	6.26	5.01	1.02	1.61	0.95
C(12)	0.9536	0.4776	0.3654	6.34	6.62	7.03	1.34	4.42	0.82
C(13)	0.9754	0.4115	0.5153	3.66	7.78	8.78	1.86	2.58	2.28
C(21)	0.8360	0.6932	0.3614	6.51	5.66	9.48	−2.62	1.51	0.94
C(22)	0.9555	0.6743	0.4294	5.12	8.39	18.19	−6.21	−5.62	2.66
C(23)	0.9510	0.6168	0.4785	4.58	5.81	8.65	−2.58	1.09	0.94
C(31)	0.4378	0.6772	0.0803	7.26	8.73	6.81	0.18	3.11	1.62
C(32)	0.4630	0.6433	0.0002	9.32	11.51	6.11	0.13	1.12	−0.20
C(33)	0.5856	0.6177	0.0513	6.92	4.95	5.25	0.26	2.09	0.93
C(41)	0.3405	0.6302	0.4460	7.32	5.44	3.97	−1.27	1.85	−0.40
C(51)	−0.0199	0.6063	0.0545	4.49	4.79	5.29	2.14	1.61	0.13
C(52)	0.0310	0.6279	−0.0234	3.46	5.03	5.29	1.42	−0.09	1.58
C(53)	0.0197	0.5974	−0.1114	4.80	5.85	4.52	0.23	0.86	−0.40
C(54)	0.0710	0.6176	−0.1806	6.82	6.48	5.45	1.82	1.29	2.02
C(55)	0.1304	0.6701	−0.1611	5.24	9.45	8.43	0.60	1.26	4.01
C(56)	0.1440	0.7035	−0.0793	6.77	5.11	6.89	0.35	0.18	2.17
C(57)	0.0969	0.6826	−0.0060	5.44	6.01	6.99	2.57	−1.21	0.85
C(61)	0.2902	0.4800	−0.0451	6.05	5.14	4.74	−0.41	3.06	−0.17
C(62)	0.3177	0.4336	−0.1112	4.85	4.61	3.37	−0.07	2.31	0.81
C(63)	0.4247	0.4036	−0.0782	3.69	5.08	5.54	0.10	2.15	0.19
C(64)	0.4456	0.3592	−0.1393	6.99	7.00	4.70	1.06	3.45	−0.36
C(65)	0.3633	0.3469	−0.2378	8.67	7.17	5.62	0.80	4.71	−0.13
C(66)	0.2541	0.3781	−0.2708	5.44	7.33	3.57	−1.25	0.81	−1.07
C(67)	0.2322	0.4215	−0.2089	5.12	5.98	4.84	−1.25	2.02	0.26
C(71)	0.3187	0.2564	0.1405	11.19	4.09	9.28	−1.89	4.17	−0.49
C(72)	0.2543	0.2625	0.0228	10.82	3.33	11.09	−2.52	2.38	−2.25
C(73)	0.2153	0.3255	0.0050	6.03	3.50	5.70	−1.18	1.57	−2.07
C(81)	0.7165	0.2963	0.4513	4.61	7.39	7.27	4.76	2.15	2.07
C(82)	0.7785	0.2691	0.3821	9.53	14.96	5.72	7.01	4.08	2.66
C(83)	0.7266	0.2988	0.2814	8.13	11.65	7.08	4.96	3.95	2.14
C(91)	0.3000	0.4071	0.4812	3.05	6.32	4.80	−0.05	2.50	−0.80
C(92)	0.2154	0.3759	0.3919	3.30	5.00	5.73	0.57	2.39	0.27
C(93)	0.1739	0.3966	0.2936	3.51	5.62	5.91	0.54	2.44	−0.71
C(94)	0.0887	0.3678	0.2060	4.51	6.62	7.81	0.11	2.73	−1.75
C(95)	0.0494	0.3139	0.2280	4.05	7.48	9.25	−0.95	2.08	−1.34

Table II (*Continued*)

Atom	x	y	z	B_{11}	B_{22}	B_{33}	B_{12}	B_{13}	B_{23}
C(96)	0.0923	0.2894	0.3245	5.40	6.78	11.25	−0.39	3.09	−0.85
C(97)	0.1736	0.3216	0.4099	4.45	4.68	8.99	0.42	3.01	1.20
C(101)	0.7546	0.4283	0.7909	6.01	5.66	4.01	−0.38	2.04	−0.94
C(102)	0.8060	0.3716	0.7766	4.33	5.75	2.64	−0.60	0.00	0.75
C(103)	0.7381	0.3193	0.7599	5.14	6.06	6.34	−1.41	2.02	0.16
C(104)	0.7864	0.2675	0.7459	8.59	5.19	6.99	−0.14	2.25	−0.52
C(105)	0.9027	0.2632	0.7472	5.29	5.96	7.65	0.42	1.60	−0.28
C(106)	0.9704	0.3126	0.7638	3.73	7.89	8.22	0.71	1.40	1.89
C(107)	0.9253	0.3666	0.7798	4.71	6.25	7.20	−1.21	1.14	1.68
N(A1)	0.6451	0.4642	0.1711	5.42	7.48	5.21	−0.74	2.72	−0.73
C(A11)	0.6989	0.4557	0.1247	5.83	12.37	5.14	−1.42	2.68	−1.94
C(A12)	0.7782	0.4420	0.0657	8.76	25.19	11.76	−3.07	6.53	−5.79
N(A2)	0.5938	0.0437	0.2538	9.47	16.45	10.67	−0.79	4.83	−1.81
C(A21)	0.6923	0.0634	0.3054	11.94	22.96	7.36	−2.82	5.57	−2.17
C(A22)	0.8077	0.0668	0.3678	10.67	21.35	9.49	−3.62	4.60	−3.10
N(A3)	0.3089	0.1066	0.1873	10.25	13.03	11.15	−1.30	4.74	0.32
C(A31)	0.2976	0.1215	0.2633	12.54	9.08	9.74	−0.47	5.68	0.28
C(A32)	0.2882	0.1316	0.3616	10.34	10.94	11.65	−1.76	5.13	−2.56

[a] The first 40 atoms after Br^- and Li^+ are the backbone atoms $C_i^{\alpha}C_i'N_iO_i$ of the ten peptide groups, the following 44 atoms are those in the side groups where $C_i^{\beta} = C(i1)$, $C_i^{\gamma} = C(i2)$, etc., and the last nine atoms belong to the three CH_3CN molecules. [b] The thermal parameters are expressed in the form $T = \exp[-1/4(B_{11}h^2a^{*2} + B_{22}k^2b^{*2} + B_{33}l^2c^{*2} + 2B_{12}hka^*b^* + 2B_{13}hla^*c^* + 2B_{23}klb^*c^*)]$ where the B_{ij} values are in $Å^2$ units.

Table III. Bond Lengths (Å) and Angles (deg)

Angles	i = 1	2	3	4	5	6	7	8	9	10	Av i = 1–10	Av for polypeptides[16]
$C_{i-1}'N_iC_i^{\alpha}$	120.7	119.2	123.8	120.8	119.1	121.6	118.7	129.1	116.3	122.1	121.1	122
$N_iC_i^{\alpha}C_i'$	106.3	112.9	111.0	113.8	114.1	108.2	111.1	108.3	110.8	112.1	110.9	111
$C_i^{\alpha}C_i'N_{i+1}$	118.3	121.4	113.5	119.5	116.8	116.4	114.7	112.6	120.0	116.0	116.9	116
$C_i^{\alpha}C_i'O_i$	121.3	117.6	121.7	115.9	121.2	122.9	119.1	122.9	116.3	118.2	119.7	120.5
$N_{i+1}C_i'O_i$	120.4	120.9	124.8	124.6	122.1	120.4	126.1	124.1	123.6	125.8	123.3	123.5
$C_i'C_i^{\alpha}C_i^{\beta}$	110.6	111.2	111.3	108.6	110.1	111.4	110.1	108.5	112.4	112.7		
$N_iC_i^{\alpha}C_i^{\beta}$	109.1	105.5	99.6	110.5	111.1	104.9	102.7	105.5	105.9	113.2		
Bonds	Val	Pro	Pro	Ala	Phe	Phe	Pro	Pro	Phe	Phe		
N_i–C_i^{α}	1.493	1.432	1.471	1.464	1.474	1.472	1.464	1.447	1.496	1.438	1.465	1.455
C_i^{α}–C_i^{β}	1.590	1.511	1.498	1.478	1.561	1.576	1.581	1.595	1.562	1.531	1.548	
C_i^{α}–C_i'	1.518	1.524	1.583	1.567	1.499	1.490	1.589	1.538	1.540	1.572	1.542	1.51
C_i'–O_i	1.237	1.240	1.231	1.206	1.217	1.189	1.217	1.240	1.253	1.233	1.226	1.24
C_i'–N_{i+1}	1.350	1.330	1.334	1.324	1.387	1.377	1.337	1.354	1.333	1.312	1.344	1.325

Table IV. Conformational Angles[11] in Lithium Antamanide·CH_3CN

i	Val 1	Pro 2	Pro 3	Ala 4	Phe 5	Phe 6	Pro 7	Pro 8	Phe 9	Phe 10
ϕ_i	−115	−65	−81	−69	−84	−123	−74	−69	−79	−90
ψ_i	138	139	148	−13	−6	140	145	145	−13	8
ω_i	179	−4	−174	175	−178	−172	−3	−175	172	173
χ_i^1	−68, 170	12	22		66	−176	25	−21	−60	59
χ_i^2					84, −95	−87, 94			−56, 125	88, −93

Table V. Hydrogen Bonds

	Length, Å
Intramolecular	
O(3)···HN(6)	3.06
O(8)···HN(1)	3.00
Interionic	
Br^-···HN(4)	3.31
Br^-···HN(9)	3.30

membered ring is enhanced by the formation of six smaller rings using the intra-ring hydrogen bonds and the Li···O ligands as bridges (Figure 1, middle view). Atoms O(3) and O(8) play multiple roles in that they form ligands to the Li^+ as well as participate in intra-ring hydrogen bonds.

Individual values for bond lengths, Table III, have relatively high standard deviations, about 0.017 Å, owing to the termination of the least-squares refinement after one cycle of anisotropic refinement and the omission of 87 hydrogen atoms; however, the average of ten values for each type of bond is more reliable than single values and can be compared to the average values observed for small peptides[16] (six or fewer residues). Bond lengths in antamanide appear to be 0.01–0.03 Å larger for the N–C^{α}, C^{α}–C′, and C′–N bonds and

(16) See, *e.g.*, R. E. Marsh and J. Donohue, *Advan. Protein Chem.*, 22, 235 (1967).

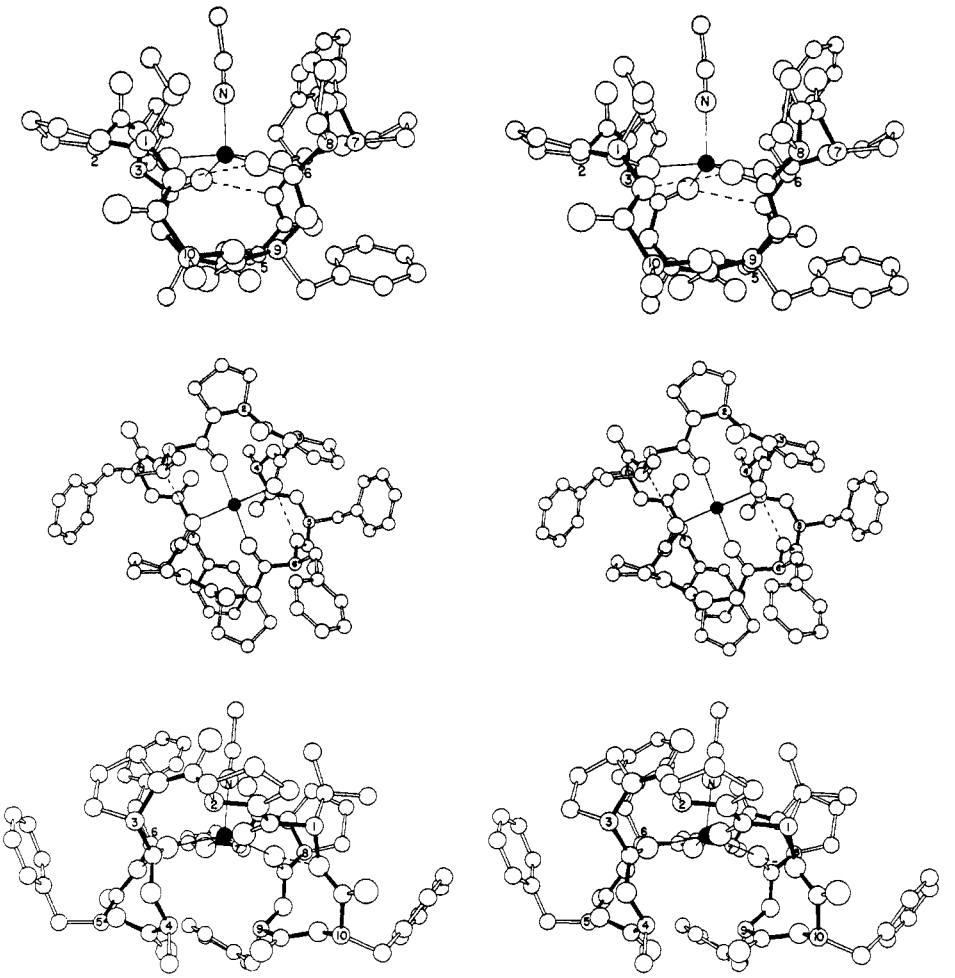

Figure 1. Stereodiagrams depicting the conformation of the lithium antamanide·CH_3CN complex. The bonds in the 30-membered polypeptide ring are darkened, the numbers refer to the C^{α} atoms in the ten residues, and Li^+ is represented by the black dot. Each view is at 90° to the other two views: (top) the phenyl groups on Phe_5 and Phe_{10} have been omitted for clarity; (middle) the CH_3CN group has been omitted; (bottom) the complete complex. The diagrams were drawn from the crystallographic coordinates by a computer program (C. K. Johnson, Oak Ridge National Laboratory).

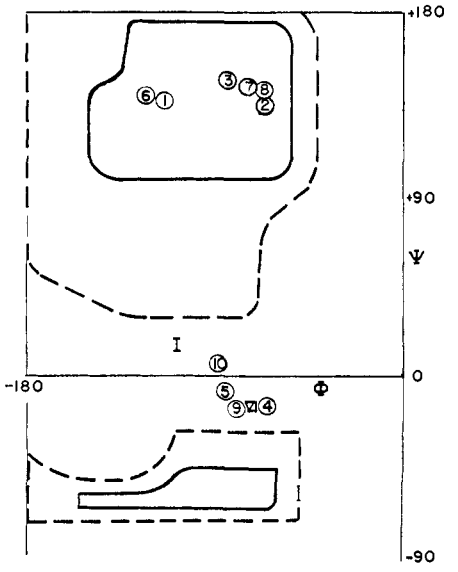

Figure 2. Conformational map. The numbers enclosed in circles refer to the ten residues in lithium antamanide·CH_3CN while the Roman numerals refer to the residues in a 1 → 4 hydrogen bond in *cyclo*(4Gly-2-D-Ala). The dashed lines enclose the areas representing low energy regions while the solid lines enclose the lowest energy areas.

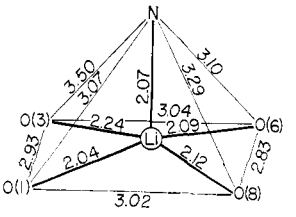

ANGLES	DEG.
O(1)LiO(3)	86
O(3)LiO(6)	89
O(6)LiO(8)	84
O(8)LiO(1)	93
NLiO(1)	96
NLiO(3)	108
NLiO(6)	96
NLiO(8)	104

Figure 3. The distances and angles for the ligands to the pentacoordinated Li^+.

0.015 Å smaller for the C=O bonds. No differences have been observed between the bond lengths in the cis and trans peptide units.

Bond angles have been reported to be different for cis and trans peptide units in cyclotetrasarcosyl[17] and in a cyclotetradepsipeptide,[12] for example, with both the $C^{\alpha}C'N$ and $C'NC^{\alpha}$ angles larger in the cis peptide group. In antamanide, there are several angular values associated with Pro_3 and Pro_8 which are significantly different than those for the remaining eight peptide groups, Table III. The $C'NC^{\alpha}$ angle for the cis Pro_2–Pro_3 linkage and the cis Pro_7–Pro_8 linkage averages near 126°, as compared to 120° for the average of

(17) P. Groth, *Acta Chem. Scand.*, 24, 780 (1970).

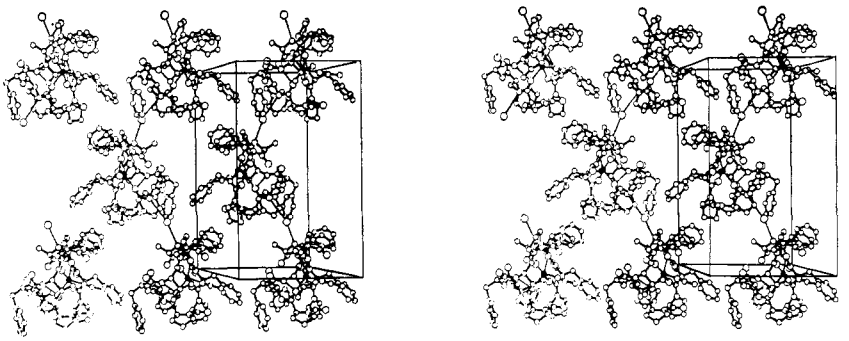

Figure 4. Packing of the Li^+-antanamide complex. The axial directions are $c \rightarrow$, $b \uparrow$, and a directed away from the viewer. Hydrogen bonds between the Br^- ion and the complexes are indicated by light lines. Solvent molecules, other than the one forming part of the complex, have been omitted.

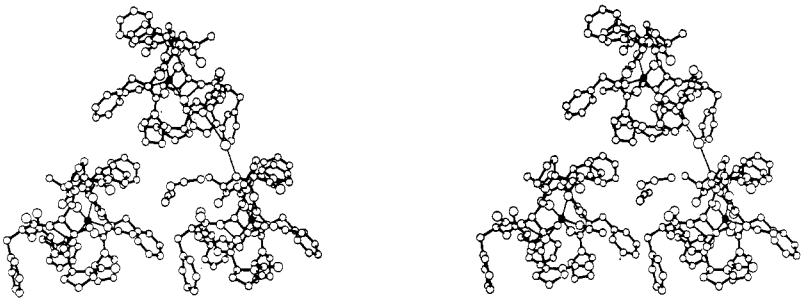

Figure 5. The three molecules in the lower right region of Figure 4 are reproduced along with the two CH_3CN solvent molecules found in the channel formed by the three molecules.

the eight trans linkages. Values of $\sim 124°$ have been reported in cyclotetrasarcosyl[17] and cyclotetradepsipeptide.[12] In addition, the $C_3^{\alpha}C_3'N_4$ and $C_8^{\alpha}C_8'N_9$ angles are $\sim 5°$ smaller than the average for the remaining $C^{\alpha}C'N$ angles; however, these angles are not in the cis peptide groups but in the groups adjacent to the cis peptide linkages.

Side Groups. Antamanide has two pairs of adjacent prolyl residues which are connected by cis peptide linkages. In the adjacent prolyl residues, the planes of the five-membered rings are approximately perpendicular to each other. Furthermore the average planes of Pro_2 and Pro_7 are approximately perpendicular to the Li···N ligand while the average planes of Pro_3 and Pro_8 are approximately parallel to the Li···N ligand. Each pyrrolidine ring has an envelope conformation. In Pro_2, Pro_7, and Pro_8, atoms C^{δ}, N, C^{α}, and C^{β} are in a plane, the largest deviation from planarity in any of the three groups being 0.04 Å, while atom C^{γ} is 0.23–0.53 Å out of the plane of the other four. However, in Pro_3, it is atom C^{β} which is 0.31 Å out of the plane of the other four. In each of the four prolyl groups, the thermal parameters for C^{γ} are considerably larger than for the other four atoms of each ring (see C(22), C(32), C(72), and C(82) in Table II). Thus there may be some disorder with the rings assuming both envelope conformations, *i.e.*, C^{γ} may be either above and below the plane of the other four atoms in disproportionate amounts.

Three of the phenylalanyl residues (5, 9, and 10) are at the bottom of the complex, as viewed in Figure 1, and the phenyl groups are folded up so as to make a more globular molecule. The χ^1 torsional angle about C^{α}–C^{β} is $+66$ and $+59°$ for the Phe_5 and Phe_{10} and $-60°$ for Phe_9, *i.e.*, the C^{β}–C^{γ} bonds are gauche with respect to the N–C^{α} bonds. The remaining phenylalanyl residue (6) is near the top of the molecule and has a χ^1 angle of $-176°$ (trans) while the two χ^1 angles for valine are $+170$ and $-68°$. Residues Val_1 and Phe_6 are oriented in such a manner as to keep the top of the cavity for the Li^+ quite open. All the χ_i^1 angles are near ± 60 or 180°, values which have usually been found for side chains[15] except, of course, in prolyl residues. For the phenylalanyl residues, the χ_i^2 torsional angles, about the C^{β}–C^{γ} bonds, are near $\pm 90°$ for three of them and near -60, $+120°$ for Phe_9. Thus, in no case is the plane of the phenyl ring near the same plane as the $C^{\alpha}C^{\beta}C^{\gamma}$ atoms.

Packing. There are two molecular complexes in the unit cell which are related by a twofold screw axis parallel to the y direction. The Br^- ion is located between the complexes and participates in two hydrogen bonds, N(4)H···Br^- with the complex below and N(9)H···Br^- with the complex above. Thus the hydrogen bonding with the Br^- ion forms an infinite chain of molecules parallel to the y direction. There is no other intermolecular hydrogen bonding. Figure 4 shows several parallel chains of molecules from adjacent unit cells. It is apparent that the packing of the antamanide complex creates a clathrate, with large channels parallel to the a axis. There are only ten van der Waals' contacts of less than 3.70 Å between the complexes. They are principally between the phenyl group of Phe_5 and O_2 or O_{10} of neighboring molecules, and between the CH_3 groups of Val_1 and O_4 or Phe_9 of adjacent molecules. Actually the closest intermolecular contact is 3.06 Å between the CH_3 group of the acetonitrile moiety and O(5) of the molecule related by $1 + x$.

The large voids in the lattice are occupied by two additional CH_3CN molecules as shown in Figure 5. Exclusion of these two solvent molecules from the structure factor calculation increases the R factor from

9.0 to 11.2%. Careful inspection of the difference map at $R = 9.0\%$ shows that the only peaks present are those attributed to H atoms and that there are no other solvent molecules in the lattice. Each end of the two solvent molecules has two van der Waals' contacts (3.1–3.7 Å) with atoms in the host molecules.

Discussion

The alkali metal ion complex of antamanide is most stable in a lipophilic environment.[2] The nature of the folding of the residues of the complex is understandable in terms of the above observation. The cup in which the Li^+ resides is rimmed with the hydrogen atoms from four pyrrolidine rings, the isopropyl moiety of Val_1 and the tolyl moiety of Phe_6. In addition, the hole in the top of the complex is plugged by a CH_3CN solvent molecule and the CH_3 group of that molecule completes the hydrophobic surface. The lower half of the molecule is surrounded by phenyl groups, thus continuing the hydrophobic surface. Of the six NH groups available for hydrogen bonding, two participate in *intra*molecular bonds in the interior of the molecule, two make hydrogen bonds with the Br^- ions, while the remaining two NH groups, N(5) and N(10), are so effectively shielded by the hydrophobic side groups that they do not participate in hydrogen bonding. Thus the almost completely hydrophobic surface of the globular complex should facilitate its movement through the lipid layers of cell membranes.

A comparison of the conformation of the Li^+–antamanide complex with the K^+–nonactin complex[18] and the K^+–valinomycin complex[19] (preliminary results) shows several differences. In both K^+ complexes, the K^+ occupies the center of the complex and is symmetrically surrounded by six or eight O atoms with $K\cdots O$ distances ranging from 2.7 to 2.8 Å. Furthermore, the nonactin ring folds into a figure resembling the seams of a tennis ball with very nearly $\bar{4}$ symmetry and completely encases the K^+. The valinomycin, containing both D and L residues, forms a thick doughnut shaped ring around the K^+ and has nearly $\bar{3}$ symmetry. The Li^+–antamanide, on the other hand, has much less symmetry, only an approximate twofold axis, and much bulkier side groups. Moreover, the Li^+ resides in a relatively shallow cup with all ligands from the ion to the antamanide moiety on one side of the Li^+. The other side of the Li^+ is strongly coordinated to a solvent molecule.

Curiously, there is another cavity in the molecule located below the Li^+ which remains empty. The lower cavity is lined with six carbonyl O atoms, O(1), O(3), O(6), and O(8) which coordinate with the Li^+ in the upper cavity and O(4) and O(9) in addition. The intramolecular $O(4)\cdots O(9)$ distance is 3.76 Å, $O(9)\cdots O(8)$ is 3.88 Å, and all other $O\cdots O$ approaches involving O(4) or O(9) are larger. The question arises as to why the Li^+ ion is attracted to the upper open cavity rather than the lower cavity.

The spectroscopic data of Faulstich, *et al.*,[4] show that uncomplexed antamanide in polar solvents in the presence of H_2O has a conformation similar to that of the Na^+ complex. If uncomplexed antamanide is already folded into a conformation close to that described here for the Li^+ complex, then it is plausible that the upper open cavity is much more accessible to the Li^+ ion than the lower cavity which is surrounded by the bulky hydrophobic side groups of Phe_5, Phe_9, and Phe_{10} as well as the CH_3 of Ala_4.

Acknowledgment. I wish to express my appreciation to Drs. Th. Wieland, H. Faulstich, and W. Burgermeister of the Max Planck Institute für Medizinische Forschung, Heidelberg, for providing the crystals and to Dr. B. Witkop of the National Institutes of Health for helpful discussions. This project was supported in part by the Office of Naval Research Project Order P04-0095 and in part by the NIAMD of the National Institutes of Health.

(18) B. T. Kilbourn, J. D. Dunitz, L. A. R. Pioda, and W. Simon, *J. Mol. Biol.*, **30**, 559 (1967).
(19) M. Pinkerton, L. K. Steinrauf, and P. Dawkins, *Biochem. Biophys. Res. Commun.*, **35**, 512 (1969).

Communications to the Editor

Intramolecular Rearrangement in Olefin–Tetracarbonyliron Complexes. Importance of Olefin Rotation on the Barrier for Rearrangement

Sir:

Although the fluxional nature of five-coordinated transition metal complexes is receiving a great deal of attention,[1] the study of the rearrangement in $Fe(CO)_5$ and its derivatives, a potentially large class of fluxional molecules, is being frustrated, except in a few cases,[2] by the apparently low activation barriers involved.[3] In our quest to find an $L\cdot Fe(CO)_4$ system amenable to a variable temperature nmr study, the explanation offered by Muetterties, *et al.*,[5] to account for the contrasting fluxional behavior between amino- and thiophosphoranes and other XPF_4 type molecules seemed particularly relevant and exciting. By comparing the free energy of activation due to P–N bond rotation to that due to the rearrangement barrier (permutation of

(1) (a) P. Meakin and J. P. Jesson, *J. Amer. Chem. Soc.*, **95**, 7272 (1973); (b) J. R. Shapley and J. A. Osborn, *Accounts Chem. Res.*, **6**, 305 (1972).
(2) J. D. Warren and R. J. Clark, *Inorg. Chem.*, **9**, 373 (1970); (b) J. D. Warren, M. A. Busch, and R. J. Clark, *ibid.*, **11**, 452 (1972); (c) L. Kruczynski and J. Takats, *J. Amer. Chem. Soc.*, **96**, 932 (1974).
(3) (a) The ^{13}C nmr spectrum of $Fe(CO)_5$ is a single sharp line down to *ca.* $-170°$.[1a] (b) The intramolecular rearrangement in $Fe[(CH_3)_2PCH_2CH_2P(CH_3)_2]Fe(CO)_3$ is still rapid at $-80°$.[4]
(4) M. Akhtar, P. D. Ellis, A. G. MacDiarmid, and J. D. Odom, *Inorg. Chem.*, 11, 2917 (1972).
(5) E. L. Muetterties, P. Meakin, and R. Hoffman, *J. Amer. Chem. Soc.*, **94**, 5674 (1972).